SUPPLEMENTARY INFORMATION

Inhibiting cancer metabolism by aromatic carbohydrate amphiphiles that act as antagonists of the glucose transporter GLUT1

Alexandra Brito,[a-d] Patrícia M. R. Pereira,[c] Diana Soares da Costa,[a,b] Rui L. Reis,[a,b,e] Rein V. Ulijn,[d,f,g] Jason S. Lewis,[c,h-k] Ricardo A. Pires,[a,b,e*] and Iva Pashkuleva,[a,b*]

[a]3B's Research Group, I3Bs - Research Institute on Biomaterials, Biodegradables and Biomimetics, University of Minho, Headquarters of the European Institute of Excellence on Tissue Engineering and Regenerative Medicine, AvePark, Parque de Ciência e Tecnologia, Zona Industrial da Gandra, 4805-017 Barco, Guimarães, Portugal; [b]ICVS/3Bs - PT Government Associate Laboratory, Braga/Guimarães, Portugal; [c]Department of Radiology, Memorial Sloan Kettering Cancer Center, New York, NY 10065, USA; [d]Advanced Science Research Center (ASRC) at the Graduate Center, City University of New York (CUNY), 85 St Nicholas Terrace, New York, New York 10031, USA; [e]The Discoveries Centre for Regenerative and Precision Medicine, Headquarters at University of Minho, Avepark, 4805-017 Barco, Guimarães, Portugal; [f]Department of Chemistry, Hunter College, City University of New York, 695 Park Avenue, New York 10065, USA; [g]PhD programs in Biochemistry and Chemistry, The Graduate Center of the City University of New York, New York 10016, USA; [h]Department of Radiology, Weill Cornell Medical College, New York, NY 10065, USA; [i]Molecular Pharmacology Program, Memorial Sloan Kettering Cancer Center, New York, NY 10065, USA; [j]Department of Pharmacology, Weill Cornell Medical College, New York, NY 10065, USA; [k]Radiochemistry and Molecular Imaging Probes Core, Memorial Sloan Kettering Cancer Center, New York, NY 10065, USA

E-mails: rpires@i3bs.uminho.pt; pashkuleva@i3bs.uminho.pt

Experimental procedures

Synthesis and purification of the aromatic N-glucosides (1b-d). The compounds 1b-d were obtained from the respective glucosamines using previously described one-step synthetic procedure.[1-3] Briefly, the sodium salt of the glucosamine was dissolved in water (30 g/L) in the presence of 2 eq sodium hydrogen carbonate (Riedel-de Haen, Germany) and reacted with 1.5-2 eq 9-fluorenylmethoxycarbonyl chloride (Fmoc-Cl, Sigma, Germany) dissolved in dioxane until complete consumption of the respective glucosamine (detected by TLC). The product was purified by column chromatography (230-400 mesh silica gel) to remove the non-reacted Fmoc (eluent EtOAc:MeOH:H2O, 5:3:2 for 1b, c and 7:2:1 for 1d). The purified compounds were fully characterized by HPLC, MS and NMR (Fig. S1-S3).

Molecular docking. The identification of potential binding sites of 1a-d to GLUT1 was performed by an automated molecular-docking procedure using the web-based SwissDock program.[4, 5] The GLUT1 structure was uploaded from Protein Data Bank website, 4PYP (Crystal structure of the human glucose transporter GLUT1).[6] The structure of the tested ligands 1a-d was uploaded in Mol2 format. The docking was performed using CHARMM Force Field with EADock DSS and default parameters, i.e. the whole target protein structure was considered.[4, 7] The prediction of the binding modes and subsequent calculation were performed with UCSF Chimera software.[8]

Cell culture. SaOs2 human osteosarcoma and MDA-MB-468 mammary gland/breast cancer cell lines were purchased from American Type Culture Collection (ATCC). The cell lines were authenticated at Memorial Sloan-Kettering Cancer Center (MSKCC) integrated genomics operation core using short tandem repeat analysis. The cells used in our experiments were mycoplasma free and had a passage number lower than 15. SaOs2 were cultured at

37 °C in a humidified 95/5% air/CO_2 atmosphere using Dulbecco's modified Eagle's medium (DMEM) low glucose (Sigma) supplemented with 10% fetal bovine serum (FBS, Gibco, UK) and 1% antibiotic/antimycotic (Gibco, UK) solution. In the case of MDA-MB-468 cells, we used the same procedure but replaced DMEM low glucose with DMEM high glucose (Sigma).

Flow cytometry. SaOs2 and MDA-MB468 were detached with PBS/4mM EDTA. After centrifugation (250 g, 5 min) cells were re-suspended in PBS and incubated for 45 min at 4 °C with rabbit anti-human GLUT1 antibodies and anti-human β-actin antibody, following manufacturer-recommended concentrations. Cells were subsequently washed with PBS, centrifuged, and incubated with secondary antibody alexa fluor 488 during 45 min at 4 °C. Cells were washed again with PBS, centrifuged and fixated in 1% formalin in PBS. Data acquisition was performed on a FACS Calibur Flow Cytometer (BD Biosciences) and analyzed using the Flowing Software v2.5.1.

Supplementation of cell cultures with aromatic N-glucosides (1b-d). All solutions were prepared just before the use. A concentration of 0.5 mM of the compounds 1b, d was prepared by dissolving them in the corresponding cell culturing media and were supplemented to cell monolayers formed after 24 h of cell seeding. Due to the poor solubility in aqueous media, compound 1c was dissolved in dimethyl sulfoxide (DMSO) at concentration of 1 M and then was diluted in the respective cell culture media to a final concentration of 0.5 mM. For all the experiments, the concentration of DMSO was kept under 0.005%.

Immunofluorescence analysis of glucose transporter 1 (GLUT1). Anti-Glucose transporter GLUT1 (rabbit polyclonal antibody) was purchased from Abcam®. Cells were fixed in 1% formalin for 3 min, permeabilized with 0.2 % TritonX-100 for 5 min and blocked in 3% bovine serum albumin in phosphate buffered saline (PBS) at room temperature for 30 min. Cells were incubated with the primary anti-GLUT1 antibody overnight at 4 °C. After washing, secondary antibody incubation was performed with an anti-rabbit IgG Alexa-Fluor-488 for 30 min at room temperature. Phalloidin–Tetramethylrhodamine (TRITC) conjugate was used (1:200 in PBS for 30 min, Sigma) to assess cytoskeleton organization. Nuclei were counterstained with 1 μg/mL 4,6-4,6-diamidino-2-phenyl (DAPI, Sigma) for 30 min. The cells were washed with PBS, mounted with Vectashield® (Vector) in glass slides and observed under an Imager Z1 fluorescence microscope (Zeiss) and photographed using an Axio Cam MRm (Zeiss).

Real-Time Polymerase Chain Reaction. Total RNA extraction was performed using TRIzol ® reagent. Chloroform was added to the cell extract and centrifuged at 12 000 *g* for 10 min. The aqueous phase was separated from the organic one and the RNA was recovered from it by precipitation with isopropyl alcohol. One μg of total RNA was transcribed to cDNA (cDNA quantification kit). RT-PCR analysis of the samples was performed in triplicate. Oligonucleotide primer pairs were used to detect the presence of mRNAs encoding members of the GLUT family (SLC2A) in ATDC5, SaO2 and MDA-MB-468 cell lines by real time RT-PCR. Fragments were analyzed by agarose gel electrophoresis. The oligonucleotides sequences are presented below.

Oligo name	Sequence (5' → 3')	Tm (°C)	MW (g/mol)
HsGlut1Fwd	TCCACGAGCATCTTGAGA	56.7	5773
HsGlut1Rev	ATACTGGAAGCACATGCCC	56.7	5782
HsGlut2Fwd	CACTGATGCTGCATGTGGC	58.8	5820
HsGlut2Rev	ATGTGAACAGGGTAAAGGCC	57.3	6215
HsGlut3Fwd	TTCAAGAGCCCATCTATGCC	57.3	6037
HsGlut3Rev	GGTCTCAGGGACTTTGAAGA	57.3	6197
HsGlut4Fwd	GGCATGTGTGGCTGTGCCATC	63.7	6469
HsGlut4Rev	GGGTTTCACCTCCTGCTCTAA	59.8	6348
Hs18SFwd	CCCCTCGATGCTCTTAGCTG	57.3	6116
Hs18SRev	CCCATCACGAATGGGGTTCA	57.3	6135

Glucose uptake assay. NBDG was used as a direct method for visualization and quantification of Glc uptake following previously established protocols.[9, 10] Briefly, cells (50 000 cells/cm^2) were seeded on tissue culture polystyrene coverslips. 24 h after seeding, the culture medium was removed and the cells were incubated with 0.02 mM NBDG for 30 min and then were washed with Krebs'–Ringer HEPES (KRH) buffer pH 7.4, containing the following (in mM): 136 NaCl, 20 HEPES, 4.7 KCl, 1.25 $MgSO_4$ and 1.25 $CaCl_2$. The samples were then analyzed under laser scanning confocal microscopy (Leica, TCS SP8).

Lactate production. Intra- and extracellular lactate production was assessed using the Lactate Assay Kit (Sigma-Aldrich, MAK064). SaOs2 or MDA-MB-468 cells were collected by scraping the wells and centrifuge at 2 000 *g* for

10 min at 4 °C. The supernatant was collected and used to quantify the extracellular lactate. The cell pellet was homogenized in 0.25 M metaphosphoric acid solution, in ice for 5 min followed by centrifugation (10 000 *g* for 5 min at 4 °C) and neutralization with 5 M potassium carbonate (K_2CO_3) solution. Additional centrifugation (10 000 *g* for 5 min at 4 °C) was performed to remove insoluble material and the supernatant was used to quantify the intracellular lactate. A master reaction mix containing 20 µL sample solution, 100 µL lactate assay buffer, 20 µL of lactate cofactor mixture and 20 µL fluorometric substrate was added, followed by addition of 40 µL of lactate dehydrogenase and reactions were incubated at RT for 20 min. Sample fluorescence was measured using an excitation wavelength of 530-540 nm and an emission wavelength of 585-595 nm, on a microplate reader.

Metabolic activity (MTS assay). Cells metabolic activity was assessed by MTS (CellTiter 96® AQueous One Solution) following the supplier's instructions. The optical density (OD) was read at 490 nm on a multiwell microplate reader (Synergy HT, BioTek Instruments). The metabolic activity is presented as a ratio between the values obtained for the cells cultured in the presence of 0.5 mM of **1b-d** and the control (values obtained in the absence of the compounds).

Viability assay (alamarBlue). Cells in exponential growth phase were seeded in 96 well plate at a density of 50 000 cells/cm^2 and incubated overnight at 37 °C and 5 % carbon dioxide (CO_2). The culture medium was then removed and replaced by medium without FBS containing **1b-d** with concentrations ranging from 3 mM – 0.125 mM. The cells were incubated at 37 °C and 5 % CO_2 for 24 h. After this time, 10 µL of alamar blue were added to each well. The cells were incubated again for 3 h at 37 °C and 5 % CO_2. The fluorescence with an excitation wavelength at 530-560 nm and emission wavelength at 590 nm was then measured in a microplate reader (SYNERGY HT, Manufacturer Biotek). Medium with **1b-d** but without cells was used as a negative control. Untreated cells were used as positive control. The viability and the IC_{50} was calculated according to the manufacturer's instructions.[11]

Proliferation assay. Quantification of cell proliferation was performed with Quan-iT™ PicoGreen® dsDNA assay kit (Molecular Probes/Invitrogen) after cell lysis following the manufacturer's instructions. The effect of the **1b-d** on cell proliferation was also assessed by the Ki-67 immunohistochemistry (rabbit monoclonal antibody, Abcam). Briefly, cells were fixed in 1 % formalin for 3 min, permeabilized with 0.2 % TritonX-100 for 5 min and blocked in 3 % bovine serum albumin in PBS at room temperature for 30 min. Ki-67 antibody incubation was performed overnight at 4 °C. Nuclei were counterstained with 1 µg/mL 4,6-diamidino-2-phenyl (DAPI, Sigma) for 30 min. Samples were washed with PBS, mounted with Vectashield® (Vector) in glass slides and observed under a laser scanning confocal microscopy (Leica, TCS SP8).

NBDG fluorescence quantification. The pictures were recorded as described in glucose uptake experimental part. The green channel (NBDG) was converted to gray scale, then each image was divided in smaller images to optimize the threshold and separate the green signal from the background. Further, the area occupied by the green signal was then calculated by the Cell Profiler 3.0 Software. For each condition 6 individual images were analyzed and the total area occupied by the green signal was normalized by the total number of cells, in each picture.

Concomitant saturation binding experiments. The experiments were performed following the protocol described elsewhere.[12] Briefly, SaOs2 or MDA-MB-468 cells were seeded (16 000 cells/well) in a 96 well plate. After 24 hrs, the cultures were supplemented with NBDG (0 – 20 nM in Krebs-Ringer-Henseleit buffer, containing 120 mM NaCl, 4.7 mM KCl, 1.2 mM $MgCl_2$, 2.2 mM $CaCl_2$, and 10 mM Hepes, pH adjusted to 7.4 with Tris). The aromatic N-glucosides **1b-d** (0.5 mM) were added to the same solution. The cells were washed with PBS after 30 min and lysed with NaOH (0.2 N, 150 µl/well, 30 min). The lysate was neutralized with HCl (0.2 N, 150 µl/well) and the fluorescence was measured in a microplate reader (467 nm excitation/542 nm emission). The obtained values were normalized to the cell number to obtain the total NBDG binding, which was plotted vs. the concentration of NBDG. The data were fit via non-linear regression with a one-site binding model in GraphPad Prism 7.00 to determine the number of the occupied GLUT1 (Bmax), the dissociation constant (Kd) and the non-specific binding component. The non-specific component was subtracted from the total NBDG binding to generate the specific binding curves.

Transfection assays. GLUT1 was depleted using a pool of three target-specific 19–25 nt siRNA (Santa Cruz Biotechnology).[13] Cancer cells were transfected upon 60–80% confluence with either SLC2A1-siRNA or scrambled (scr) siRNA (controls). Each transfection was performed for 5 h with 2.4 µM of siRNA in transfection medium (Santa Cruz) containing 0.5 µL/cm^2 of transfection reagent (Santa Cruz). After incubation with siRNA, a complete media was added for 24 h in the case of MDA-MB-468 and for 48 h for SaOs2 cultures.

Western Blot analysis. Whole protein extracts were prepared by washing cells twice with ice-cold PBS and harvesting with radioimmunoprecipitation assay buffer (RIPA buffer: 150 mM NaCl, 50 mM Tris-HCl, pH 7.5, 5 mM ethylene glycol tetraacetic acid (EGTA), 1% Triton X-100, 0.5% sodium deoxycholate (DOC), 0.1% sodium dodecyl sulfate (SDS), 2 mM phenylmethanesulfonyl (PMSF), 2 mM iodoacetamide (IAD)) and 1X protease inhibitor cocktail (Roche, Indianapolis, IN, USA). After centrifugation at 16 000 *g* for 10 min at 4 °C, supernatants were collected and used for protein quantification with Pierce BCA Protein Assay Kit (Thermo Fisher Scientific) following the manufacturer's instructions. Absorbance at 562 nm was measured on a multiwell microplate reader (Synergy HT, BioTek Instruments). Quantification was followed by denaturation of the sample with Laemmli buffer. Western Blot analysis was performed by loading 40 μg proteins per lane on 4-12% Bis-Tris Protein Gels (Novex). After electrophoresis and transfer to nitrocellulose membranes (Thermo Fischer Scientific), the membranes were incubated in 5 % (m/v) bovine serum albumin in Tris-buffered saline-Tween (TBS-T, Cell Signalling Technology) and probed with rabbit anti-GLUT1 1:1000 (rabbit polyclonal, Merck-Millipore, Watford, UK) and mouse anti β-actin 1:20 000 (Sigma) antibodies. After washing, the membranes were incubated with IRDye®800CW anti-Rabbit or anti-Mouse IgG 1:15 000 (LI-COR Biosciences) and imaged on the Odyssey Infrared Imaging System (LI-COR Biosciences) followed by densitometric analysis with ImageJ software.

Biotin pull down of cell-surface proteins. Cells were washed twice with ice-cold PBS buffer containing 0.5 mM $MgCl_2$ and 1 mM $CaCl_2$. The cell monolayers were then incubated with 0.5 mg/mL of EZ-LINK Sulfo-Biotin (Thermo Fisher Scientific) for 30 min at 4 °C with gentle rotation. The reaction was stopped by washing twice with 100 mM glycine (Thermo Fisher Scientific) in PBS containing 0.5 mM magnesium chloride ($MgCl_2$) and 1 mM calcium chloride ($CaCl_2$). Cells were scrapped in RIPA buffer, lysates were centrifuged at 16 000 *g* for 10 min at 4 °C, and supernatants were collected and assayed for protein concentration using the Pierce BCA Protein Assay Kit. A volume of 500 μL of RIPA buffer containing an equal amount of proteins was incubated with NeutrAvidin Agarose Resins (Thermo Fisher Scientific) for 2 h at 4 °C with gentle rotation and washed three times with RIPA buffer before suspension in Laemmli buffer. The total amount of the cell-surface protein content was loaded in the 4-12 % Bis-Tris Protein Gels (Novex) as described in the previous sections. In the case of the total cell lysate, 40 μg were loaded and normalization was performed by analyzing the β-actin expression.

MDA-MB-468 tumor xenografts. All animals used in this work were treated according to the guidelines approved by the Research Animal Resource Center and Institutional Animal Care and Use Committee at Memorial Sloan Kettering Cancer Center, NY. The author PMRP has a Category C accreditation for animal research given from Federation of European Laboratory Animal Science (FELASA). We adhere to the animal research: reporting of *in vivo* experiments (ARRIVE) guidelines and to the guidelines for the welfare and use of animals in cancer research. Eight- to 10-weeks-old nu/nu female mice (Charles River Laboratories) were injected subcutaneously with 1 million of MDA-MB-468 cells, in a 150 μL cell suspension of a 1:1 (v/v) mixture of medium with reconstituted basement membrane (BD Matrigel, BD Biosciences). The tumor volume (V/mm^3) was estimated by external vernier caliper measurements of the longest axis, α/mm, and the axis perpendicular to the longest axis, b/mm. The tumors were assumed to be spheroidal and the volume was calculated in accordance with the equation $V = (4\pi/3) \times (\alpha/2)2 \times (b/2)$.

Small-Animal positron emission tomography (PET) Imaging. ^{18}F-FDG (685 mCi/mmoL) was obtained from the Nuclear Pharmacy at Memorial Sloan Kettering Cancer Center on the morning of injection. **1b** was dissolved at 2 mM concentration in saline solution containing ^{18}FDG (213 - 303 μCi). To improve tumor visualization, the mice were kept fasting overnight.[14] Animals were randomly divided into two groups (n= 3 mice per group): I) NC group, tail vein co-injection of saline plus ^{18}F-FDG (200 – 205 μCi) and II) Block group, tail vein co-injection of **1b** (10 mg/kg) plus ^{18}F-FDG (200 – 205 μCi). At 30 min post injection, mice were anesthetized with 1.5 – 2 % isoflurane (Baxter Healthcare) in an oxygen gas mixture 10 min before recording PET images. The dosage (200 – 205 μCi) and the time point (30 min) for ^{18}F-FDG injection were determined according to a previous report and our preliminary studies.[15] All PET images were obtained on an Inveon PET/CT scanner (Siemens) and visualized using the AMIDE 1.0.4 software (http://amide.sourceforge.net).

Statistical analysis. Data are expressed as mean ± standard deviation. Data-set was first checked for a normal distribution using the Shapiro-Wilk normality test. Differences were analyzed by the Student t-test in the case of data with a normal distribution or by Mann-Whitney test for the sets that did not pass the normality test.

Supplementary Table 1| Complementary *in silico* data: *FullFitness* values for the top score positions and amino acids involved in the interactions between the compounds **1a-d** and GLUT1 (located at a distance below 3.5 angstroms); in parentheses is the hydrogen bonding distance, when present.

Compound	Full fitness (Kcal/mol)	Interacting residues* (distance of hydrogen bonding)
1a	-1154.34	Gly384 (1.42 Å), Gln282, Thr137, Asn288, TRp388, Glu380, Ser80, Ile164, Phe26, Asn411, Trp412, Phe379
1b	-1310.01	Trp388 (2.09Å), Glu38 (2.69Å, 1.83Å), Glu380, Phe379, Ile164, Thr137, Phe26, Gln282
1c	-1167.94	Gln161 (1.91Å), Gln282, Ile164, Phe26, Thr137, Val83, Ser80, Tyr28, Pro141, Gly138, Met142, Ala282.
1d	-1243.06	Glu380 (1.86Å), Asn317 (2.38Å), Trp388, Thr137, Ile164, Phe26, Asn411, Phe379, Trp386, Leu160, Gln280, Thr28, Gln159, Gnl282.

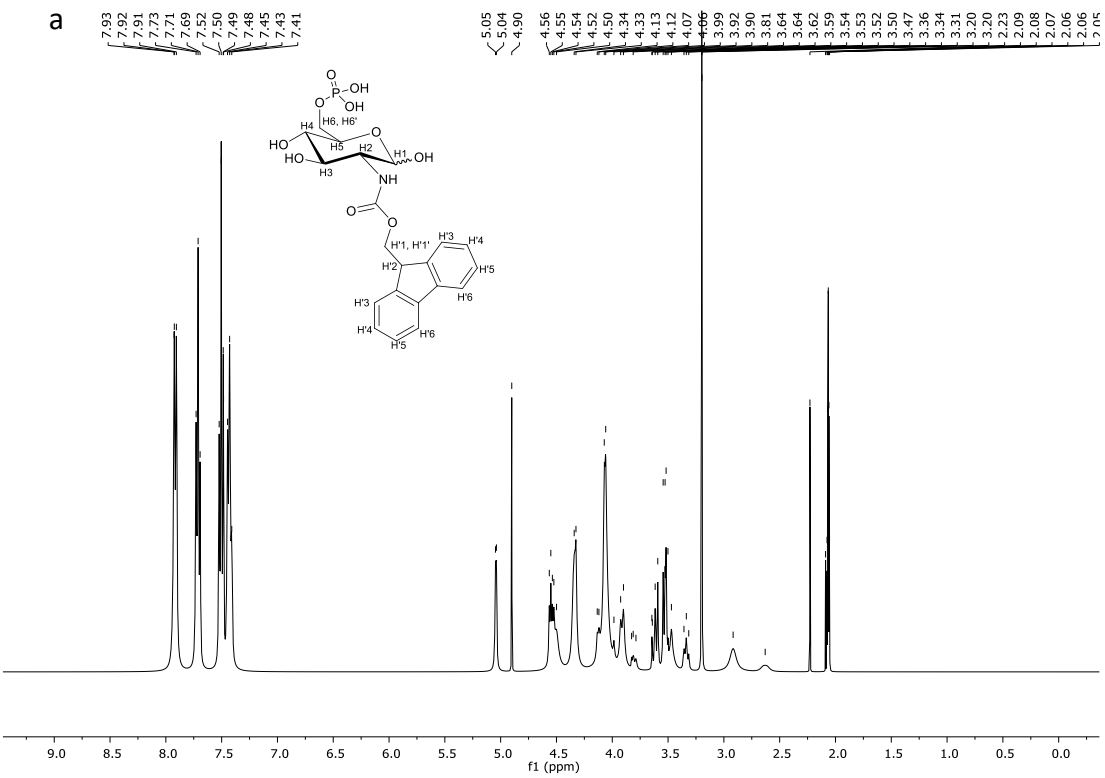
a
7.93
7.92
7.91
7.73
7.71
7.69
7.52
7.50
7.49
7.48
7.45
7.43
7.41
5.05
5.04
4.90
4.56
4.55
4.54
4.52
4.50
4.34
4.33
4.13
4.12
4.07
4.06
3.99
3.92
3.90
3.81
3.64
3.64
3.62
3.59
3.54
3.53
3.52
3.50
3.47
3.36
3.34
3.31
3.20
3.20
2.23
2.09
2.08
2.07
2.06
2.06
O
P
OH
O
OH
H6, H6'
H4
H5
H2
H1
OH
HO
HO
H3
NH
O
O
H'1, H'1'
H'3
H'4
H'2
H'5
H'6
H'3
H'4
H'5
H'6
9.0
8.5
8.0
7.5
7.0
6.5
6.0
5.5
5.0
4.5
4.0
3.5
3.0
2.5
2.0
1.5
1.0
0.5
0.0
f1 (ppm)

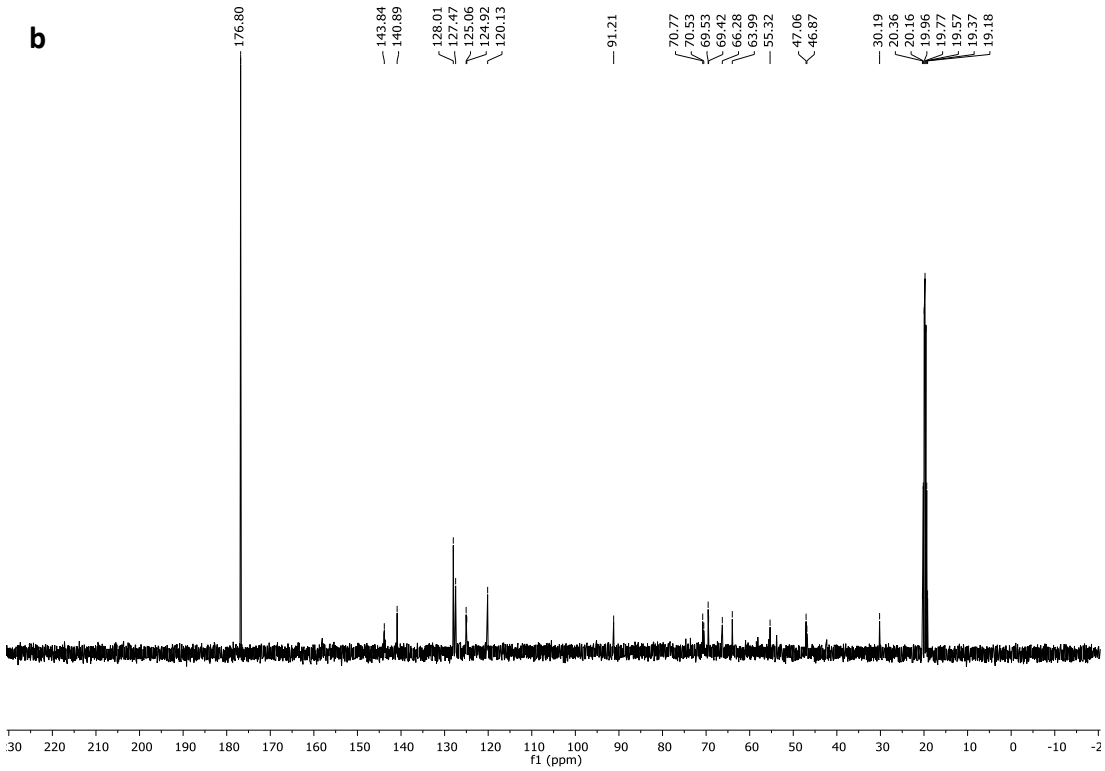
b
176.80
143.84
140.89
128.01
127.47
125.06
124.92
120.13
91.21
70.77
70.53
69.53
69.42
66.28
63.99
55.32
47.06
46.87
30.19
20.36
20.16
19.96
19.77
19.57
19.37
19.18
30
220
210
200
190
180
170
160
150
140
130
120
110
100
90
80
70
60
50
40
30
20
10
0
-10
-2
f1 (ppm)

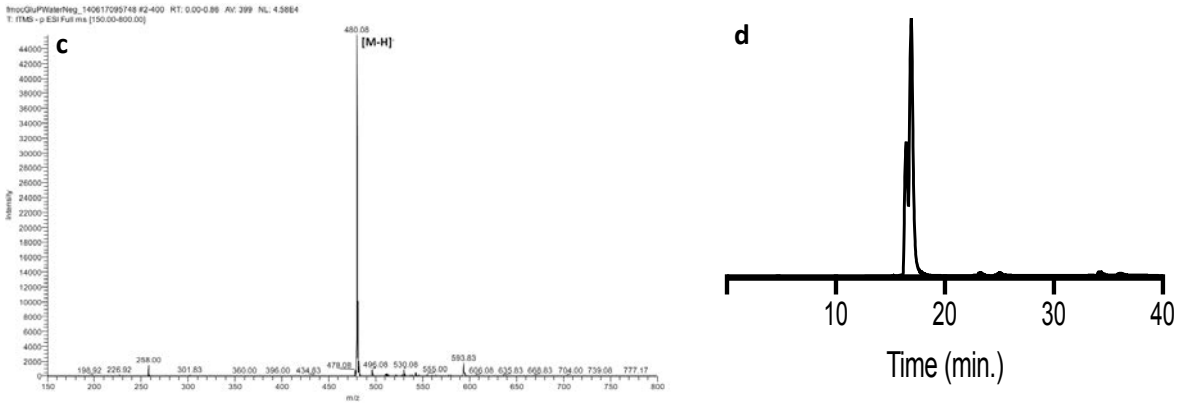

Supplementary figure S1. Characterization of fmoc-glucosamine-6-phosphate (FGlcP, **1b**): **(a)** ^{1}H NMR (400 MHz, D_2O, 298 K): δ 7.93-7.91 (dd, 2H, *J*= 8Hz; 12Hz, H'6); 7.73-7.69 (dd, 2H, *J*= 8Hz; 12Hz, H'3); 7.52-7.49 (m, 2H, H'5); 7.48-7.41 (m, 2H, H'4), 5.05 (s, 1H), 4.90 (s, 1H), 4,56 (m, 1H, H'1); 4.33 (m, 1H, H'1'), 4.12 (m, 2H, H6 + H6'), 3.90 (m, 1H, H2); 3.52 (m, 2H, H5 + H3). **(b)** ^{13}C NMR (75 MHz, D_2O, 298 K): δ 176.80, 143.84, 140.89, 128.01, 127.47, 125.06, 124.92, 120.13, 91.21, 70.77, 70.53, 69.53, 69.42, 66.28, 63.99, 55.32, 47.06, 46.87, 30.19,20.36, 20.16, 19.96, 19.77, 19.57, 19.37, 19.18. **(c)** ESI-MS spectrum of FGlcP: [M-H] 480.08; **(d)** HPLC spectrum of purified compound.

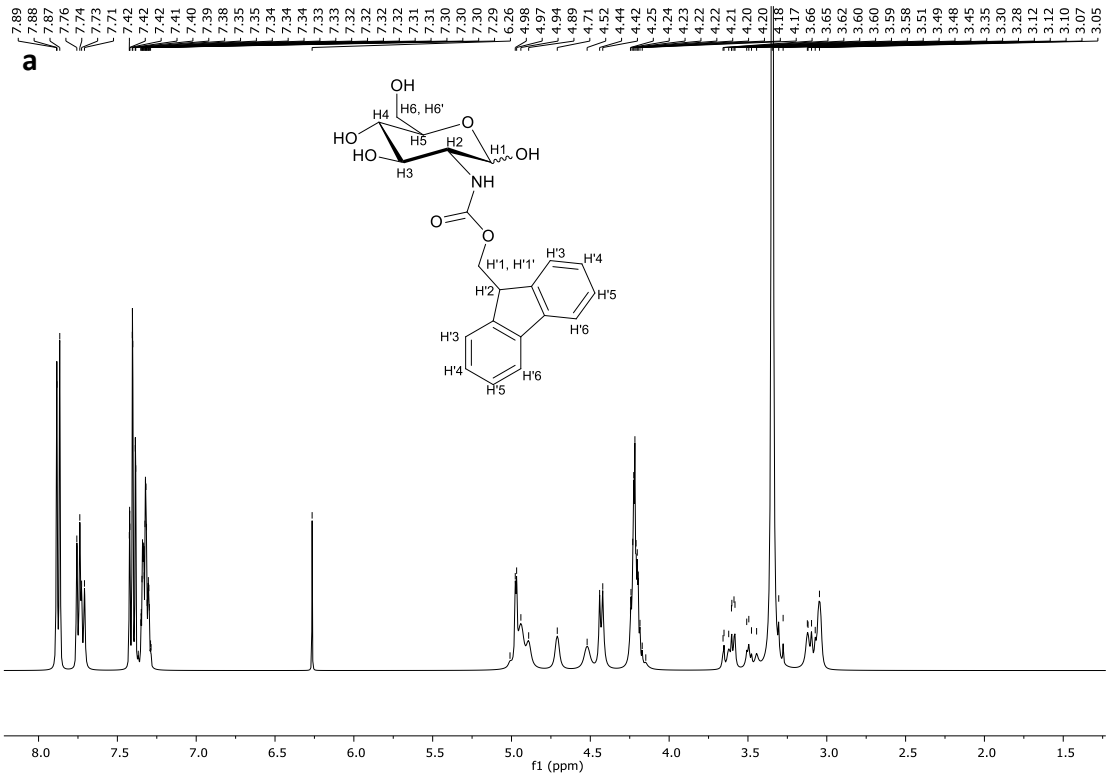
a
7.89 7.88 7.87 7.76 7.74 7.73 7.71 7.42 7.42 7.42 7.41 7.40 7.39 7.38 7.35 7.34 7.34 7.34 7.33 7.33 7.32 7.32 7.32 7.31 7.31 7.30 7.30 7.30 7.29 6.26 4.98 4.97 4.94 4.89 4.71 4.52 4.44 4.42 4.25 4.24 4.23 4.22 4.22 4.21 4.20 4.20 4.18 4.17 3.66 3.65 3.62 3.60 3.60 3.59 3.58 3.51 3.49 3.48 3.45 3.35 3.30 3.28 3.12 3.12 3.10 3.07 3.05
OH
H4
H6, H6'
O
HO
H5
H2
H1
OH
HO
H3
NH
O
O
H'1, H'1'
H'3
H'4
H'2
H'5
H'6
H'3
H'4
H'6
H'5
8.0 7.5 7.0 6.5 6.0 5.5 5.0 4.5 4.0 3.5 3.0 2.5 2.0 1.5
f1 (ppm)

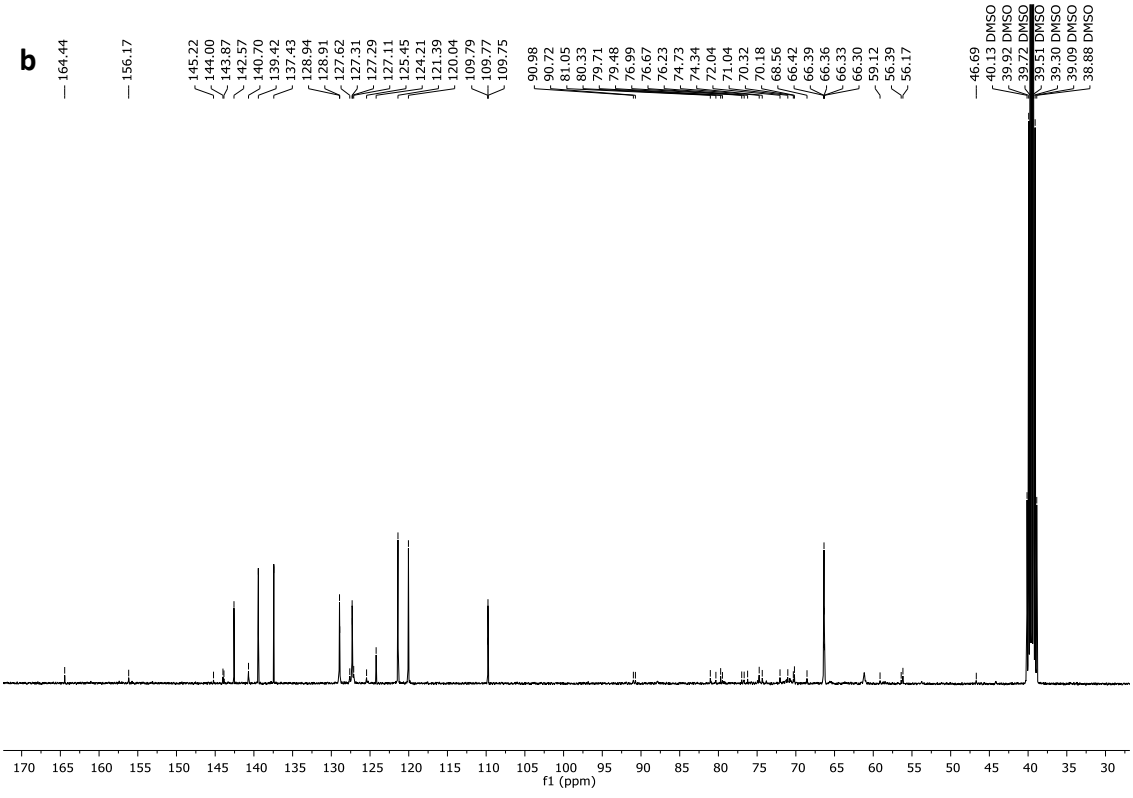
b
164.44
156.17
145.22 144.00 143.87 142.57 140.70 139.42 137.43 128.94 128.91 127.62 127.31 127.29 127.11 125.45 124.21 121.39 120.04 109.79 109.77 109.75
90.98 90.72 81.05 80.33 79.71 79.48 76.99 76.67 76.23 74.73 74.34 72.04 71.04 70.32 70.18 68.56 66.42 66.39 66.36 66.33 66.30 59.12 56.39 56.17
46.69 40.13 DMSO 39.92 DMSO 39.72 DMSO 39.51 DMSO 39.30 DMSO 39.09 DMSO 38.88 DMSO
170 165 160 155 150 145 140 135 130 125 120 115 110 105 100 95 90 85 80 75 70 65 60 55 50 45 40 35 30
f1 (ppm)

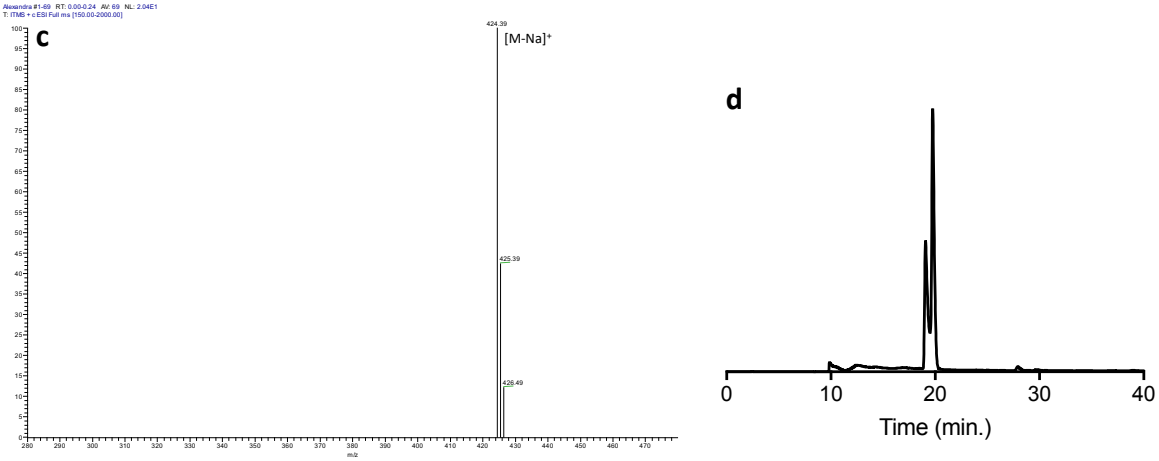

Supplementary figure S2. Characterization of fmoc-glucosamine (FGlc, **1c**): **(a)** ^{1}H NMR (400 MHz, DMSO-d_6, 298 K): δ 7.89-7.87 (dd, 2H, *J*= 8Hz; 12Hz, H'6); 7.76-7.71 (dd, 2H, *J*= 8Hz; 12Hz, H'3); 7.42-7.34 (m, 2H, H'5); 7.32-7.29 (m, 2H, H'4), 6.26 (s, 1H, OH), 4.98-4.89 (d, 1H, H'1), 4,71 (s, 1H, OH); 4.52-4.42 (s, 1H, OH), 4.25-4.23 (d, 1H, H'1'), 4.22-4.20 (m, 2H, H'2 + H4); 3.66-3.05 (m, 5H). **(b)** ^{13}C NMR (75 MHz, DMSO-d_6, 298 K): δ 164.44; 156.17; 145.22; 144.00; 143.87; 139.42; 137.43; 128.94; 127.31; 124.21; 121.39; 120.04; 90.98; 74.73; 71.04; 70.18; 68.52; 66.39; 56.39; 46.69. **(c)** ESI-MS (*m/z*) spectrum of FGlc: $[M - Na]^+$ 424.39; **(d)** HPLC spectrum of the purified compound showing the two anomers.

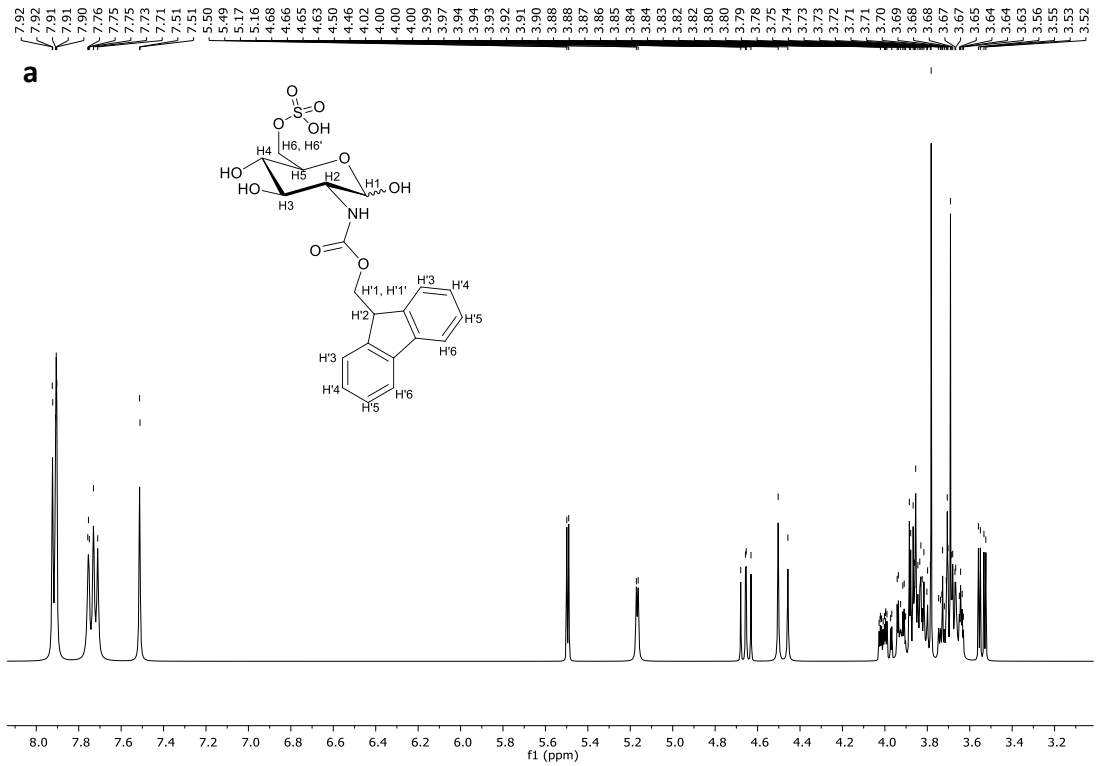
a
7.92 7.92 7.91 7.91 7.90 7.76 7.75 7.75 7.73 7.71 7.51 7.51 5.50 5.49 5.17 5.16 4.68 4.66 4.65 4.63 4.50 4.46 4.02 4.00 4.00 4.00 3.99 3.97 3.94 3.94 3.93 3.92 3.91 3.90 3.88 3.88 3.87 3.86 3.85 3.84 3.84 3.83 3.82 3.82 3.80 3.80 3.79 3.78 3.75 3.74 3.73 3.73 3.72 3.71 3.71 3.70 3.69 3.68 3.68 3.67 3.67 3.65 3.64 3.64 3.63 3.56 3.55 3.53 3.52
O
S
O
O
OH
H6, H6'
H4
H5
H2
O
H1
OH
HO
HO
H3
NH
O
O
H'1, H'1'
H'3
H'4
H'2
H'5
H'6
H'3
H'4
H'6
H'5
8.0 7.8 7.6 7.4 7.2 7.0 6.8 6.6 6.4 6.2 6.0 5.8 5.6 5.4 5.2 5.0 4.8 4.6 4.4 4.2 4.0 3.8 3.6 3.4 3.2
f1 (ppm)

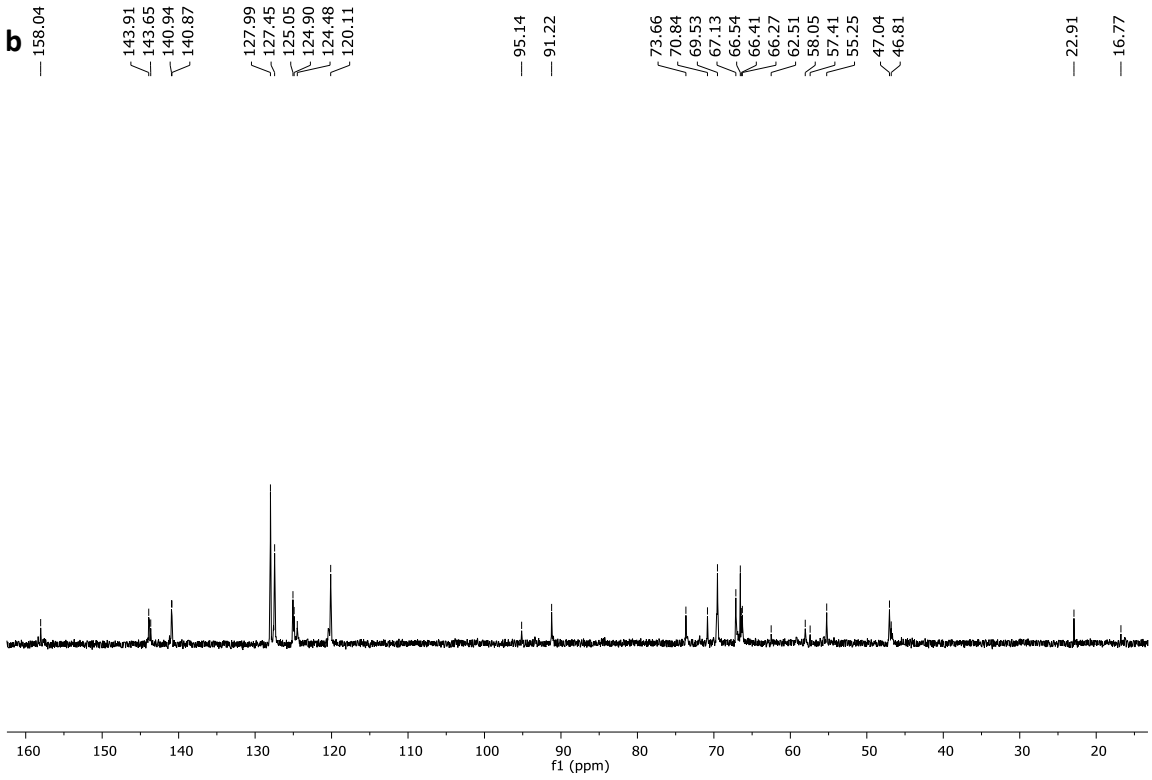
b
158.04
143.91
143.65
140.94
140.87
127.99
127.45
125.05
124.90
124.48
120.11
95.14
91.22
73.66
70.84
69.53
67.13
66.54
66.41
66.27
62.51
58.05
57.41
55.25
47.04
46.81
22.91
16.77
160 150 140 130 120 110 100 90 80 70 60 50 40 30 20
f1 (ppm)

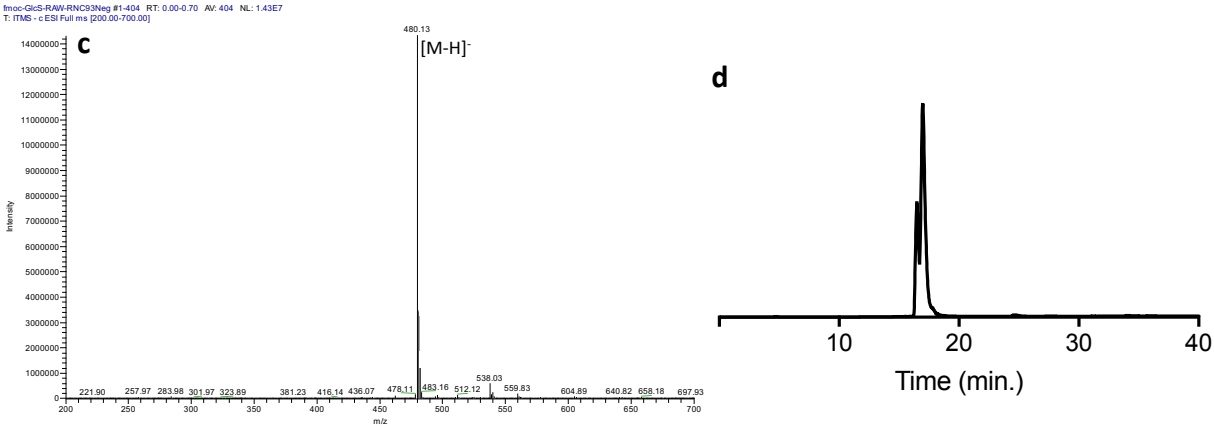

Supplementary figure S3. Characterization of fmoc-glucosamine-6-sulfate (FGlcS, **1c**): **(a)** ^{1}H NMR (400 MHz, D_2O, 298 K): δ 7.92-7.90 (dd, 2H, *J*= 8Hz; 12Hz, H'6); 7.76-7.71 (dd, 2H, *J*= 8Hz; 12Hz, H'3); 7.51 (m, 2H, H'5); 5.50-5.49 (m, 2H, H'4), 5.17 (s, 1H), 4.68 (s, 1H), 4,67 (m, 1H, H'1); 4.66 (m, 1H, H'1'), 4.46 (m, 2H, H6 + H6'), 4.02-3.94 (m, 1H, H2); 3.63-3.52 (m, 2H, H5 + H3). **(b)** ^{13}C NMR (75 MHz, D_2O, 298 K): δ 158.04; 143.91; 143.65; 140.92; 127.99; 127.45; 124.90; 120.11; 95.14; 91.22; 73.66; 70.84; 69.53; 67.13; 66.41; 62.51; 55.25. **(c)** ESI-MS spectrum of FGlcP: $[M - H]^-$ 480.13; **(d)** HPLC spectrum of purified compound

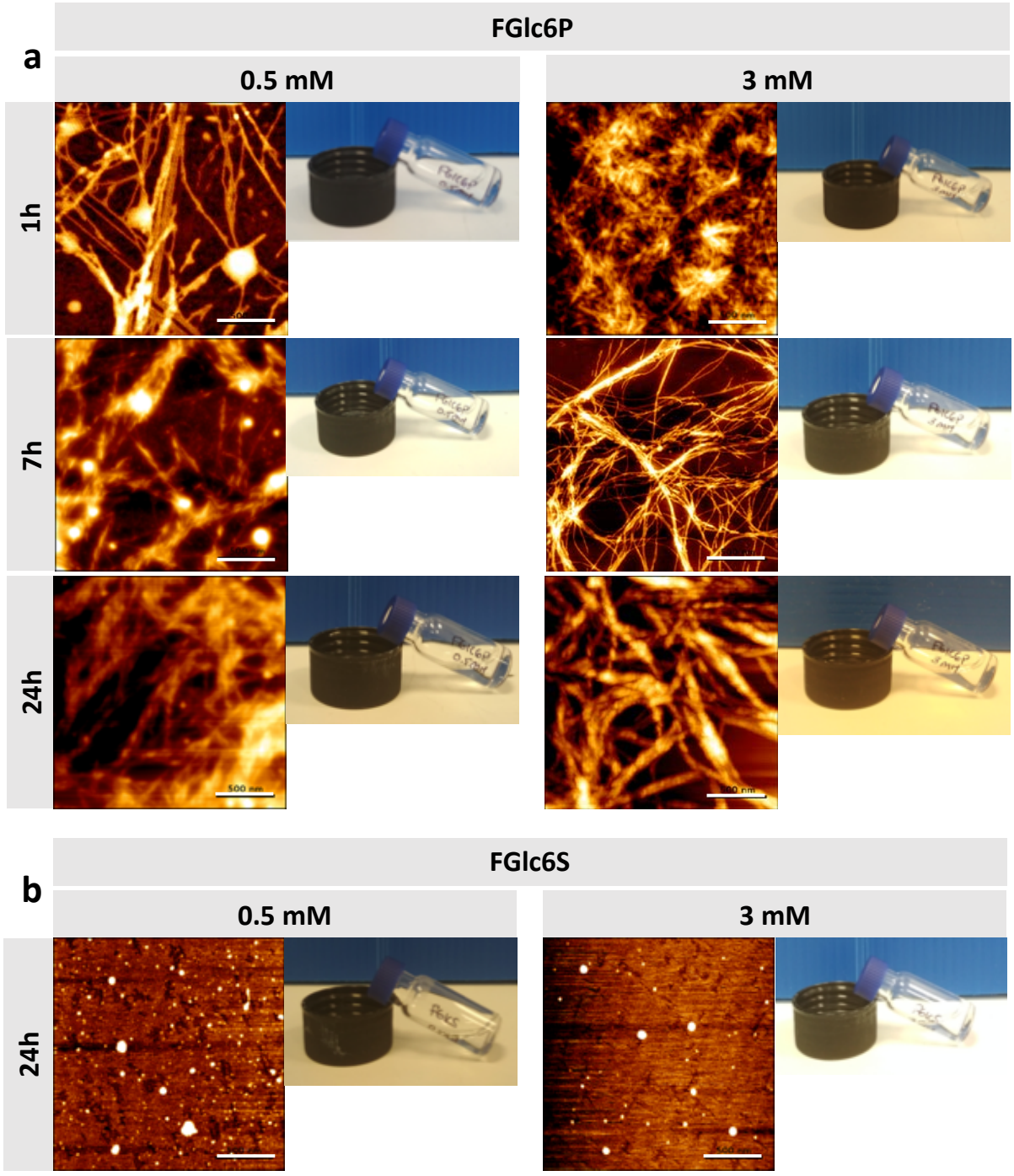

Supplementary figure S4. Atomic force microscopy images and macroscopic aspect of the aromatic N-glucosides in the presence of alkaline phosphatase (6 mU/mL, *i.e.* concentration of membrane bound ALP in SaOs2 cell lines): **(a)** The addition of the enzyme triggers formation of nanofibers when FGlcP (**1b**) is used; while **(b)** FGlcS (**1d**) does not form fibers at the studied conditions. No gelation (inverted vial test) was observed at the studied conditions but the viscosity of the FGlcP solution started to increase 7 hrs after the addition of the enzyme.

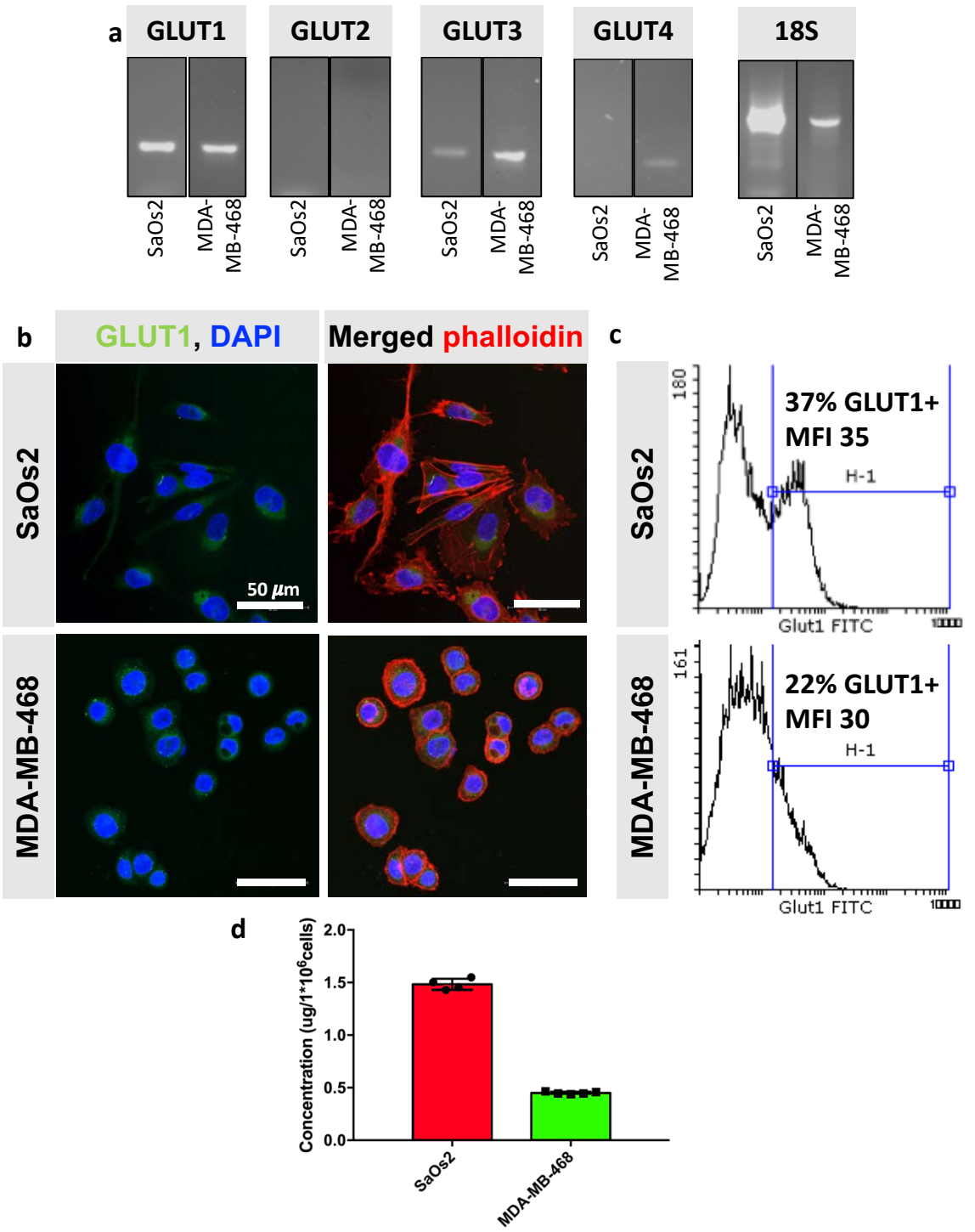

Supplementary figure S5| Characterization of the selected cancer cell lines: (a) Agarose gel electrophoresis of the PCR products for *GLUT1-4* genes coding GLUT1-4, 18S is a housekeeping gene used as a control; **(b)** Confocal microscopy images visualizing the cytoskeletal organization (phalloidin, red), cells nuclei (DAPI, blue) and GLUT1 expression (green) in of SaOs2 and MDA-MB-468; **(c)** Flow cytometry data showing the percentage of GLUT1 positive cells from the total cell population and the level of GLUT1 expression (mean fluorescent intensity, MFI); **(d)** Membranal alkaline phosphatase expressed by SaOs2 and MDA-MB-468.

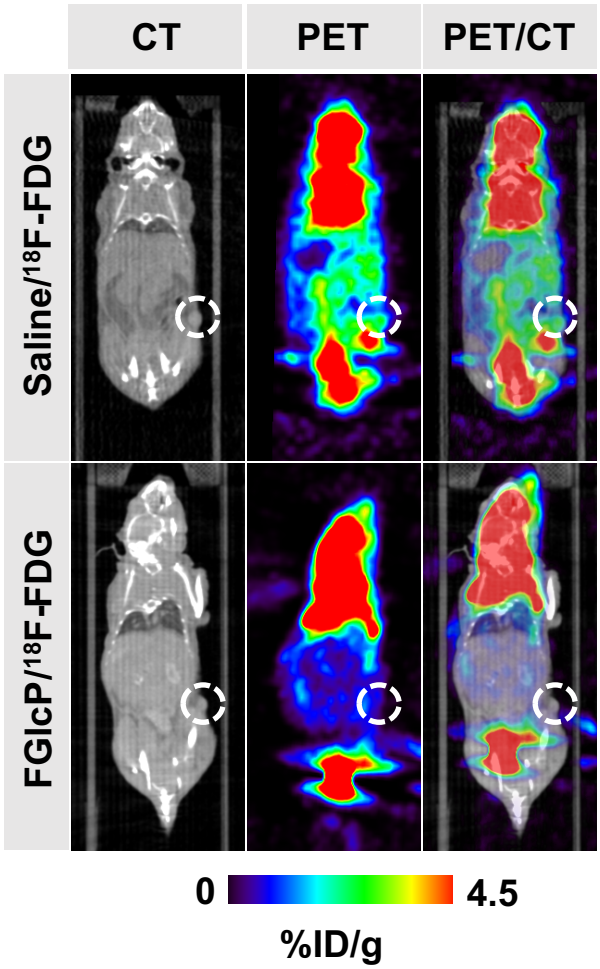

Supplementary figure S6| Aromatic N-glucoside 1b deprives glucose uptake *in vivo*: Computed tomography (CT) and positron emission tomography (PET) of fluorodeoxyglucose (^{18}F-FDG) in nude mice bearing MDA-MB-468 tumor and administrated with an excess (2 mM) of compound **1b**. Control mice were administrated with saline instead of compound **1b**.

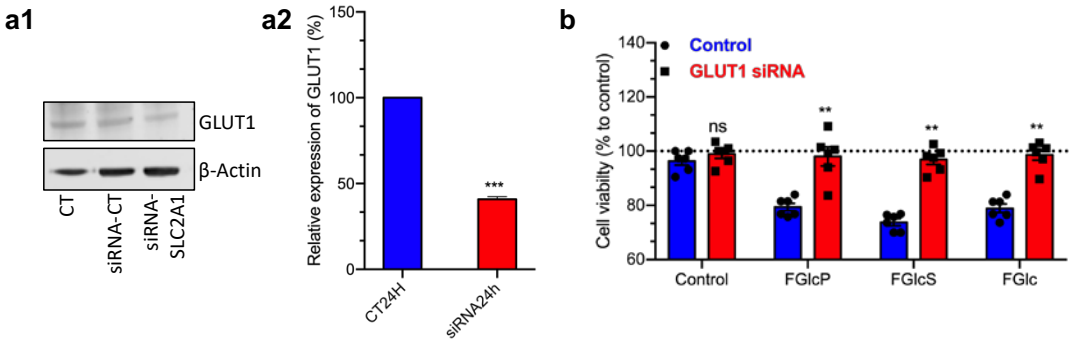

Supplementary figure S7| Relation between GLUT1 expression and the effect of aromatic N-glucosides on MDA-MB-468 viability. (a1) Representative Western blot analysis and **(a2)** the respective densitometric analysis of GLUT1 expression by MDA-MB-468 cells without transfection (CT) and after transfection with specific siRNA (siRNA-*SLC2A1*); **(b)** Cell viability of the transfected SaOs2 cells in the presence of aromatic N-glucosides **1b-d**. ns, non-significant; *: $p < 0.05$; **: $p < 0.01$; *** $p< 0.001$.

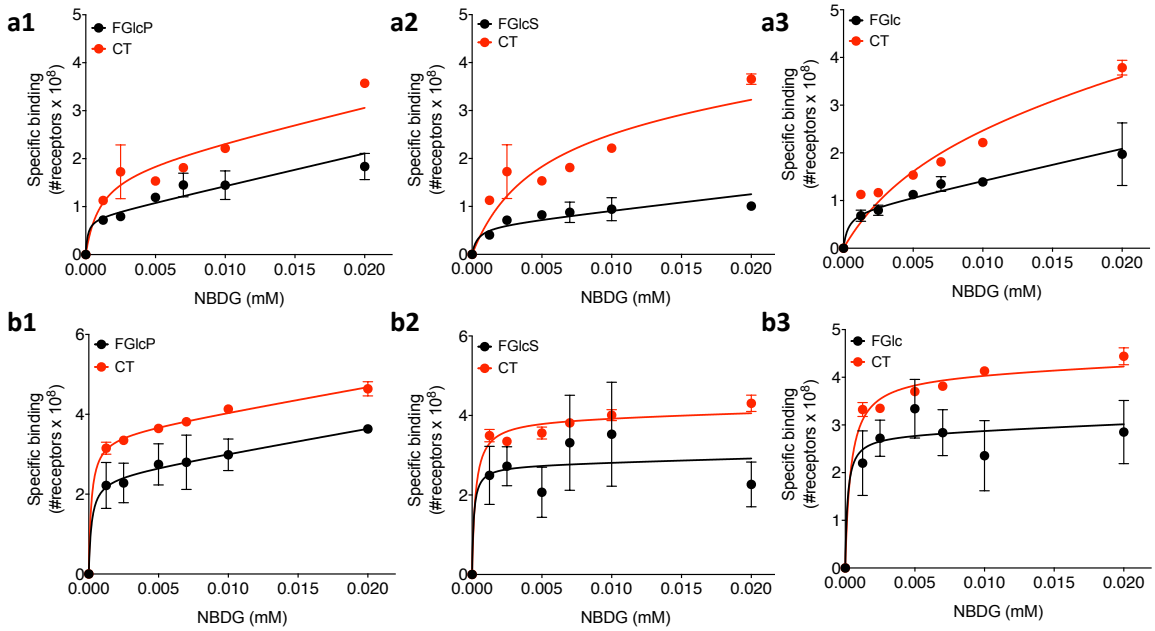

Supplementary figure S8| Specific binding of NBDG by **(a)** SaOs2 and **(b)** MDA-MB-468 in the absence (control, red) and in the presence of aromatic N-glucosides (0.5 mM, black): (a1, b1) FGlcP, (a2, b2) FGlcS and (a3, b3) FGlc. Cells were incubated for 1 h at 37 °C.

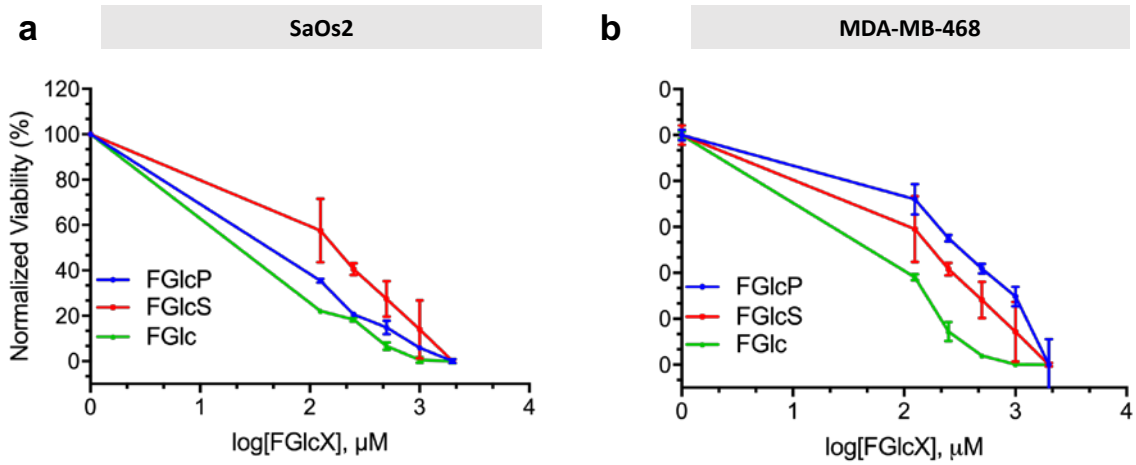

	SaOs2	MDA-MB-468
1b|FGlcP	IC_{50} = 79 µM R^2 = 9.9	IC_{50} 307 µM R^2 = 8.7
1c|FGlc	IC_{50} = 52 µM R^2 = 9.8	IC_{50} = 99 µM R^2 = 9.9
1d|FGlcS	IC_{50} = 171 µM R^2 = 9.0	IC_{50} = 404 µM R^2 = 9.5

Supplementary figure S9| IC_{50} plots and values for the aromatic N-glucosides 1b-d. (a) Viability of human osteosarcoma cell line SaOs2 in the presence of compounds **1b-d** at different concentrations (24 hrs); (**b**) Viability of human breast cancer cell line MDA-MB-468 treated with aromatic N-glucosides at different concentrations (24 hrs); **(c)** IC_{50} values obtained from the plots. All results were normalized to the control – cells cultured in the absence of aromatic N-glucosides.

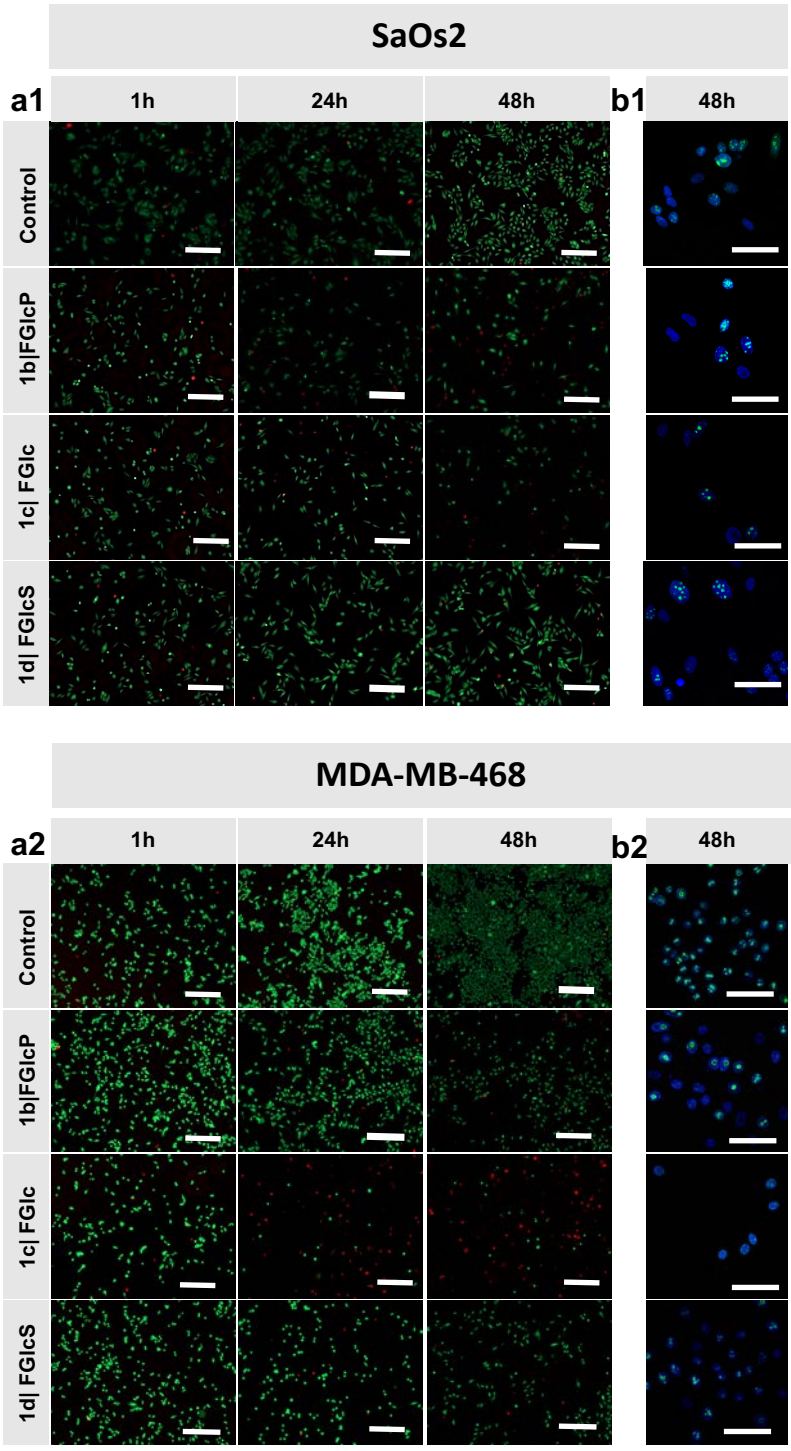

Supplementary figure S10| Effect of the compounds 1b-d on the viability and proliferation of SaOs2 and MDA-MB-468: (a) Confocal laser scanning microscopy (CLSM) images of SaOs2 (a1) and MDA-MB-468 (a2) cells supplemented with **1b-d** (0.5 mM) and stained with calcein AM (green) for live cells and propium iodide (red) for the dead ones. **(b)** CLSM images of the studied cells stained with the proliferation marker Ki67 (light blue) and DAPI (dark blue) to visualize the nuclei.

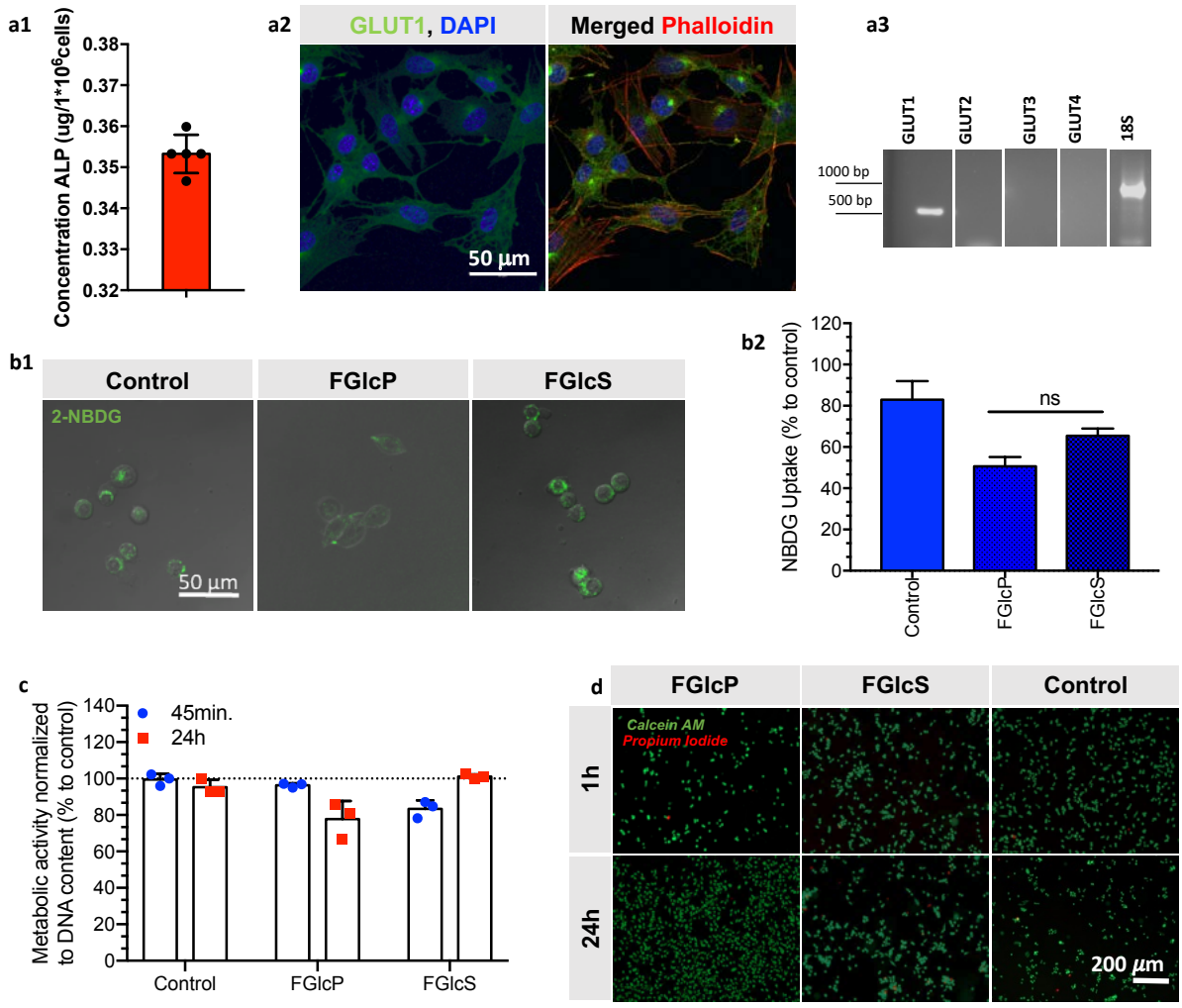

Supplementary figure S11| Effect of aromatic N-glucosamines on prechondrocyte ATDC5 cell line: (a) Expression of (a1) membrane-bound alkaline phosphatase (ALP) and (a2, a3) GLUT1 by ATDC5 showing relative low membranal ALP and mainly intracellular GLUT1; **(b)** effect of FGlcP (1b) and FGlcS (1d) on the glucose uptake: (b1) Representative fluorescent confocal scanning microscopy images showing uptake of 2-(N-(7-nitrobenz-2-oxa-1,3-diazol-4-yl)amino)-2-deoxyglucose (NBDG, green, 0.02 mM) by the ATDC5 cells in the presence of aromatic N-glucosides 1b and 1d (0.5 mM), (b2) NBDG uptake calculated from the fluorescence images; **(c)** Metabolic activity of ATDC5 after incubation with 0.5 mM aromatic N-glucosides 1b or 1d for 45 min and 24 h; **(d)** Confocal laser scanning microscopy (CLSM) images of ATDC5 cells supplemented with 1b or d (0.5 mM) and stained with calcein AM (green) for live cells and propium iodide (red) for the dead ones. Statistics were calculated using the t-test.

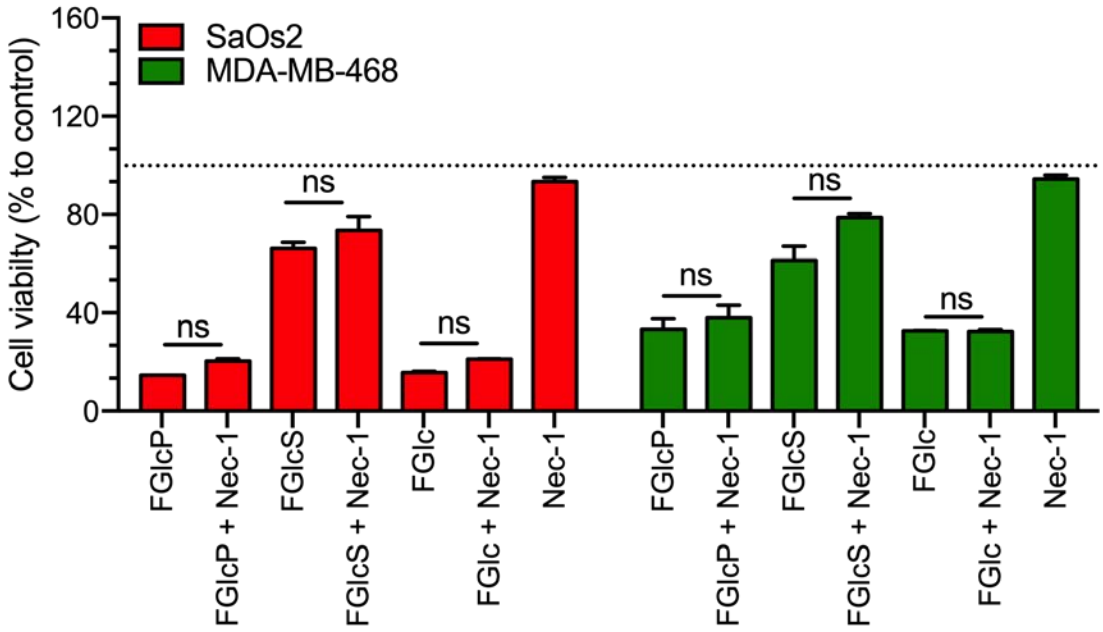

Supplementary figure S12| **Effect of the necroptosis inhibitor Nec-1 on cell viability**: cells were cultured in the presence of the compounds **1b-d** (0.5 mM) with or without the apoptosis inhibitor Z-Fa-FMK and the viability was determined after 24 hrs. The results are normalized to the control (cell culture without aromatic N-glucosides); ns: statistically non-significant difference.

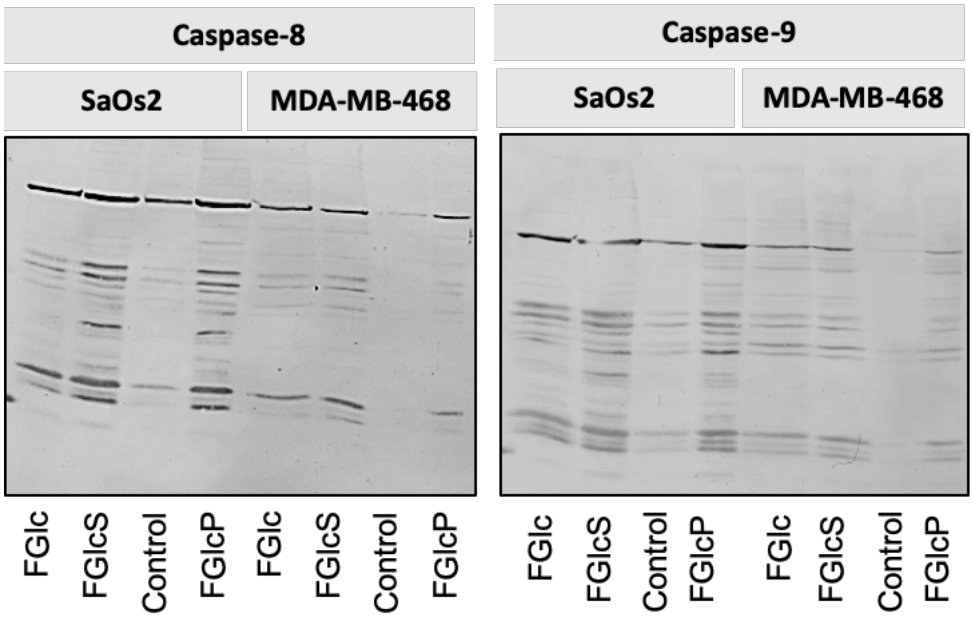

Supplementary figure S13| **Western blot analysis of initiators caspases 8 and 9** for SaOs2 and MDA-MB-468 cell lines in the presence and absence of compounds **1b-d**.

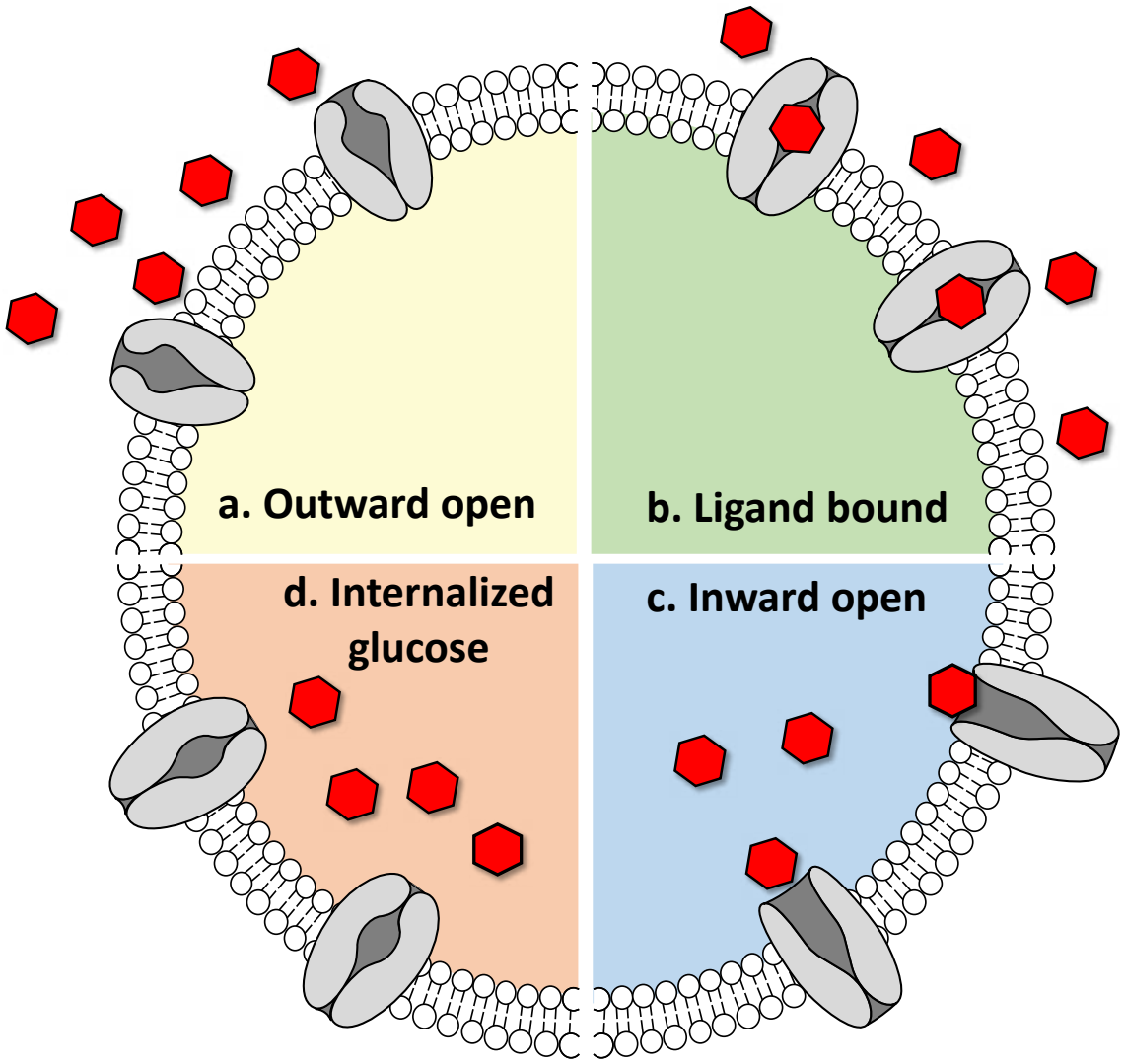

Supplementary figure S14| **Glucose (Glc) transport via GLUT1**: **(a)** Glc is internalized via several residues of transmembrane segments 1, 4, 7 and 10 (here not shown in detail) that form the outward open conformation. **(b)** The primary substrate binding (ligand-bound) induces conformational changes. **(c)** The substrate is released from the inward open conformation as it is exposed to a low concentration environment. **(d)** The Glc release induces restauration of the initial GLUT1 conformation. When Glc is replaced by aromatic-N-glucosides either the rearrangement from ligand bond to inward open conformation of the release from the inward open conformation might be compromised.

References:

1. A. Brito, Y. M. Abul-Haija, D. S. da Costa, R. Novoa-Carballal, R. L. Reis, R. V. Ulijn, R. A. Pires and I. Pashkuleva, *Chemical Science*, 2019, **10**, 2385-2390.
2. R. A. Pires, Y. M. Abul-Haija, D. S. Costa, R. Novoa-Carballal, R. L. Reis, R. V. Ulijn and I. Pashkuleva, *Journal of the American Chemical Society*, 2015, **137**, 576-579.
3. L. S. Birchall, S. Roy, V. Jayawarna, M. Hughes, E. Irvine, G. T. Okorogheye, N. Saudi, E. De Santis, T. Tuttle, A. A. Edwards and R. V. Ulijn, *Chemical Science*, 2011, **2**, 1349-1355.
4. A. Grosdidier, V. Zoete and O. Michielin, *J Comput Chem*, 2011, **32**, 2149-2159.
5. A. Grosdidier, V. Zoete and O. Michielin, *Nucleic Acids Research*, 2011, **39**, W270-W277.
6. D. Deng, C. Xu, P. C. Sun, J. P. Wu, C. Y. Yan, M. X. Hu and N. Yan, *Nature*, 2014, **510**, 121-+.
7. A. Grosdidier, V. Zoete and O. Michielin, *Proteins: Structure, Function, and Bioinformatics*, 2007, **67**, 1010-1025.

8. E. F. Pettersen, T. D. Goddard, C. C. Huang, G. S. Couch, D. M. Greenblatt, E. C. Meng and T. E. Ferrin, *Journal of Computational Chemistry*, 2004, **25**, 1605-1612.
9. K. Yamada, M. Nakata, N. Horimoto, M. Saito, H. Matsuoka and N. Inagaki, *Journal of Biological Chemistry*, 2000, **275**, 22278-22283.
10. K. Yamada, M. Saito, H. Matsuoka and N. Inagaki, *Nature Protocols*, 2007, **2**, 753-762.
11. J. L. Sebaugh, *Pharmaceutical Statistics*, 2011, **10**, 128-134.
12. P. Hein, M. C. Michel, K. Leineweber, T. Wieland, N. Wettschureck and S. Offermanns, in *Practical Methods in Cardiovascular Research*, eds. S. Dhein, F. Wilhelm Mohr and M. Delmar, Springer, Berlin, Heidelberg, 2005, DOI: 10.1007/b137833, ch. 6, pp. 723-783.
13. P. M. R. Pereira, S. Silva, J. A. S. Cavaleiro, C. A. F. Ribeiro, J. P. C. Tome and R. Fernandes, *Plos One*, 2014, **9**.
14. B. J. Fueger, J. Czernin, I. Hildebrandt, C. Tran, B. S. Halpern, D. Stout, M. E. Phelps and W. A. Weber, *Journal of Nuclear Medicine*, 2006, **47**, 999-1006.
15. R. L. Aft, J. S. Lewis, F. J. Zhang, J. Kim and M. J. Welch, *Cancer Research*, 2003, **63**, 5496-5504.